Accepted Manuscript

CO_2 Absorption Using Diethanolamine-Water Solutions in a Rotating Spiral Contactor

Jordan M. MacInnes, Ahmed A. Ayash, George R. M. Dowson

PII: S1385-8947(16)31215-3
DOI: http://dx.doi.org/10.1016/j.cej.2016.08.123
Reference: CEJ 15689

To appear in: *Chemical Engineering Journal*

Received Date: 8 June 2016
Revised Date: 4 August 2016
Accepted Date: 27 August 2016

Please cite this article as: J.M. MacInnes, A.A. Ayash, G.R. M. Dowson, CO_2 Absorption Using Diethanolamine-Water Solutions in a Rotating Spiral Contactor, *Chemical Engineering Journal* (2016), doi: http://dx.doi.org/10.1016/j.cej.2016.08.123

CO_2 Absorption Using Diethanolamine-Water Solutions in a Rotating Spiral Contactor

Jordan M. MacInnes[1], Ahmed A. Ayash and George R. M. Dowson

Chemical and Biological Engineering

University of Sheffield, Mappin Street

Sheffield S1 3JD

August 2016

Abstract

Results for mass transfer in a rotating spiral device are presented here for absorption of carbon dioxide from nitrogen carrier gas using mixtures of diethanolamine (DEA) and water. The ability of the device to examine the full range of flow rate ratio for the two phases while controlling the relative thicknesses of the phase layers is applied to surveying absorption performance over a wide range of DEA concentration at 312 K and 1.8 bara. Comparisons are made for a fixed 86 μm liquid layer thickness, which is shown to fix also the fraction of the liquid accessible by diffusion, while maintaining 90% removal of CO_2 from a gas stream of 10% (mole) CO_2 in nitrogen. The increasing liquid viscosity with DEA fraction is countered by reducing the liquid flow rate to maintain constant liquid layer thickness and diffusion depth. The allowed gas throughput, while meeting 90% removal, increases with DEA concentration until the increasing viscosity gives sufficient reduction in liquid flow rate to offset the increasing CO_2 capacity of the liquid. The maximum gas flow rate has a broad peak centred at a DEA mole fraction of about 0.072 (31% by mass). Utilisation of the amine is increased as DEA concentration increases, apparently as a result of the longer residence

[1] Corresponding author, j.m.macinnes@sheffield.ac.uk

time, suggesting an effect of chemical time scales on the order of seconds. For a fixed concentration, full utilisation of the amine is achieved by decreasing the liquid flow rate, which reduces layer thickness and increases diffusion time. The work highlights the use of the rotating spiral for rapid and accurate testing to determine optimum liquid composition of absorbent formulations.

Key words: rotating spiral, absorption, centrifugal, diethanolamine, DEA, diffusion

1. Introduction

MacInnes and Zambri [1] describe a rotating spiral device for carrying out fluid phase contacting and study its hydrodynamic characteristics for gas-liquid contacting. Measurements of liquid layer thickness over a wide range of rotation rate, gas flow rate, liquid flow rate and liquid viscosity were captured well by the 'wide channel' model of MacInnes et al. [2]. In rotating spiral contacting, gas-liquid or liquid-liquid immiscible fluids are forced by centrifugal acceleration to flow in parallel layers of approximately uniform thickness, either co-currently or counter-currently. Choice of channel height allows the throughput per device volume to be varied; adjustment of the pressure gradient along the channel and the rotation rate allows optimum ratios of the phase flow rates and layer thicknesses to be achieved. Thus, the rotating spiral has the potential for precise and efficient contacting across the wide range of possible phase and solute systems.

The rotating spiral is used here in counter-current mode to characterise the performance of water-diethanolamine (DEA) solutions for carbon dioxide absorption in the first reported application to a mass transfer process. The use of amines to remove CO_2 from a gas stream is well established but current interest is focused on identifying suitable blended amines to minimise cost. Monoethanolamine (MEA), the most common in use, is giving way to other

amine species having improved capacity and, importantly, low regeneration energy cost (Rochelle et al. [3], Raynal et al. [4]). Puxty et al. [5] tested a large number of amines using equilibrium capacity for CO_2 and initial absorption rate into a liquid sample exposed to a stream of 15% CO_2 as indicators of performance. Each aimine was tested at a single common temperature and composition. Increasingly, work is considering a few targeted amines over a range of composition and including blends of amines (Ma'mun et al. [6], Sema et al. [7], Richner et al. [8], Conway et al. [9] and Lv et al. [10]).

Methods to test performance of an amine mixture over ranges of composition require considerable effort and comparisons are complicated by the large variation in viscosity with composition that is typical. High viscosity corresponds to thicker liquid layers and lower diffusion coefficients, both of which reduce solute access to the amines in the liquid phase. The surface properties (surface tension and contact angle) also vary with composition. So tests based of absorption into stirred [10] or sparged ([5], [6]) reactors may not provide a fair basis for comparison since different blends, amines or temperatures will produce different conditions of contact between the phases due to differences in Reynolds and Weber number. Tests using laminar jets [7] or falling films [9] emphasise millisecond timescales and uniformity of bounding concentration at the interface and depths of the liquid, while the liquid layer diffusion scales are seconds and compositions vary significantly along the contacting. The rotating spiral avoids these shortcomings. High viscous stress is countered by centrifugal acceleration which both provides an effective body force on the liquid that is many times greater than gravity and may be adjusted directly by changing liquid flow rate in order to maintain suitable liquid layer thickness. For the spiral geometry and rotation rate used here, the centrifugal acceleration acting along the channel is about six times larger than gravity. Also, the spiral largely avoids effects of surface forces since a single layer of liquid is formed and, once formed, the influence of surface tension and contact angle are restricted

to menisci where the interface meets the side walls. These menisci are small provided the rotation rate is sufficiently large (as in the experiments conducted here) and the liquid layer thickness remains approximately uniform and independent of the particular surface properties. A further advantage is, as has been mentioned, that the ratios of phase layer thicknesses and flow rates are fully adjustable regardless of liquid properties, allowing the optimum associated with these two crucial parameters to be identified easily. This flexibility allows testing under conditions in which the gas is fully cleaned at the same time as the amine capacity of the liquid is fully used. The full utilisation of the liquid implies contacting times are of the order of the liquid layer diffusion time scale, as is the case under practical contacting conditions.

An existing general-purpose rotating spiral apparatus is used here to determine the CO_2 absorption performance of aqueous DEA solutions, and hence optimum concentration, at 312 K and 1.8 bara. Scaling relations are developed to allow selection of liquid flow rate so that the liquid layer thickness and diffusion depth into the liquid may be held approximately constant regardless of differences in the liquid solution viscosity.Previous work with DEA includes contacting using a packed column (Aroonwilas and Veawab [11]), a spray tower (Chakma et al. [12]) and a wetted-wall apparatus (Hu et al. [13]). Aroonwilas and Veawab [11] included DEA in a study of a number of different amines and amine blends in a 2 cm diameter column containing high-efficiency packing. The tests were at atmospheric pressure, ambient temperature and at a single amine concentration (3 kmol/m^3 in water, which for DEA is 30% by mass). Chakma et al. [12] used air-assisted atomisation of 30, 35 and 60% (mass) solutions of DEA to form small droplets and enhance the absorption of CO_2. Hu et al. [13] used a falling film over grids of fine wires in a vertical plane to measure mass transfer characteristics over a wide range of DEA composition at atmospheric pressure and ambient temperature. Gas flow rates and the method used to determine interface area are

unfortunately not indicated in the paper so the mass transfer coefficients reported cannot be used for comparison with results here. However, the results presented show a peak in absorption rate at about 40% (mass) DEA, which is higher than the 31% found here.

A brief review of the chemical mechanism involved with the reaction system is given next, followed by presentation of the relations used to quantify absorption. The necessary theoretical scaling relations are then developed, including those for scaling with viscosity of the liquid layer thickness and the characteristic diffusion depth in the liquid layer. Following this, the details of the experiment and apparatus are given and results concerning optimum contacting are presented. Results are collected first for constant liquid layer thickness and diffusion depth, so the DEA concentration giving maximum gas throughput in the device can be identified. For all conditions, the fraction of the carbon dioxide removed from the gas stream is maintained constant. Second, the effect of liquid layer thickness is examined, placing the emphasis on complete usage of the DEA.

2. Theory

The DEA-CO_2 reaction in water involves a number of series and parallel reactions having a range of rates (e.g. Rinker et al. [14]). Two reactions representing the essential character of the overall reaction system can be highlighted. First, CO_2 is converted to carbamate by formation of a zwitterion followed by deprotonation in a relatively rapid reaction represented by the combined equation:

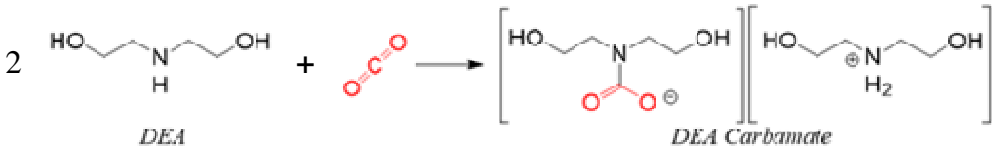

(1)

Other reactions involving water and its ionic components also form carbamate from the zwitterion with the use of just a single DEA molecule rather than two as in reaction 1. Second, water reacts with carbamate in a slow reaction that returns a DEA molecule:

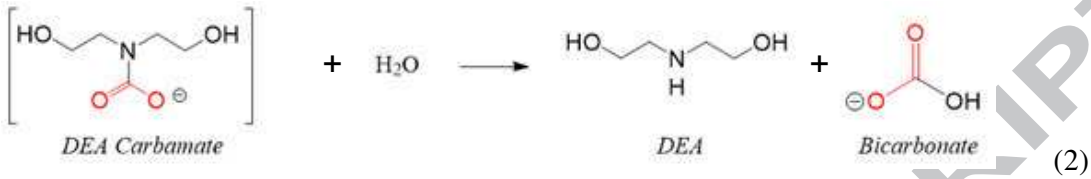

DEA Carbamate *DEA* *Bicarbonate* (2)

The equilibrium composition in the liquid adjacent to a gas of given CO_2 partial pressure can be expressed in terms of the number of moles of original unreacted DEA per CO_2 absorbed, given the symbol α. Thus, if both reactions 1 and 2 are able to progress fully to products, $\alpha = 1$ is achieved and the maximum amount of CO_2 can be absorbed for a given amount of DEA. In practice this maximum absorption will not be reached because the equilibrium is shifted towards the reactants and because insufficient time is allowed for reaction.

Data for equilibrium (Mason and Dodge [15]; Lee et al. [16]; Haji-Sulaiman et al. [17]) show that α increases with DEA concentration but decreases with CO_2 partial pressure in the gas phase. So operating at low DEA concentration and high CO_2 partial pressure reduces the amount of DEA required. From the data of Lee et al. [16] the equilibrium value of α rises from about 1.4 to 2.2 as DEA mole fraction increases from 0.01 to 0.4, at the inlet gas CO_2 mole fraction and pressure used in the experiments here.

The absorption process involves physical absorption of CO_2 at the liquid interface and diffusion of CO_2 and DEA to mix and react. The theory for one-dimensional absorption from a gas into an infinite liquid with constant solute concentration at the gas-liquid interface (van Krevelen and Howtijzer [18]; Danckwerts [19]; Gilliland et al. [20]; Brian et al. [21], Danckwerts [22]) has provided considerable insight into the process of chemical absorption. Analytical and numerical solutions show that a reaction layer forms near the liquid interface

with the reacting solute (CO_2) diffusing from the interface and the liquid reactant (DEA) diffusing from the depths of the liquid layer to meet and react. The reaction layer moves closer to the liquid interface as the reaction rate is increased relative to the inherent physical diffusion rates of the reactants. Thus, increasing the relative reaction rate produces higher absorption rate since the distance between the liquid interface and the reaction region is reduced. However, increasingly slow rate is inevitable as the amine at greater depths is accessed, the amine concentration being reduced in interface regions where CO_2 is present. Application of this theory to practical contacting typically uses a transformation from penetration with time of the reaction layer into the liquid to growth of the penetration layer with distance along the contacting length. While helpful qualitatively, this theory is not directly applicable in the conditions used here since gas concentration changes significantly with distance along the contacting length and the liquid layer has finite thickness, so that DEA may become significantly depleted. The conditions in the experiments here, according to the penetration theory, are in the pseudo first order reaction regime in which the DEA composition remains only slightly reduced in the reaction layer. That situation may hold initially but as the contacting proceeds and the DEA in the layer becomes depleted, conditions stray significantly from pseudo first order and further deviations from the theory are associated with variation of both CO_2 gas composition and DEA composition in the liquid as CO_2 is absorbed.

2.1 Absorption capacity

Even an approximate theoretical estimate of expected performance can be valuable and here the maximum possible absorption rate is estimated, both assuming perfect equilibrium between the exiting gas and the entering absorbent liquid and taking account of the reduction

from this associated with imperfect diffusional access. The absorption rate is expressed in terms of gas stream flow rate of given CO_2 composition purified to a given degree.

The maximum absorption rate of CO_2 can be estimated using mole balances on the gas and liquid phases together with the assumption that phase equilibrium is reached. The maximum absorption rate, $\dot{n}_C$, depends on the mole fraction of amine in the liquid, Y_A, the equilibrium ratio of amine to CO_2 in the liquid phase, α, and the liquid mole density, n_L, and volume flow rate, Q_L:

$$\dot{n}_C = n_L Q_L \left[\frac{Y_A}{\alpha} + \frac{Y_{Vo}}{f'} \right]$$

The second term in the brackets expresses the equilibrium mole fraction of CO_2 in the liquid when it is pure water ($Y_A = 0$). Neglecting the minor effect of water evaporation, mole balances for the gas phase of all species and of just CO_2 allow the absorption rate to be expressed alternatively in terms of the outlet gas mole density, n_V, the outlet volume flow rate, Q_V, the inlet gas CO_2 mole fraction, Y_{Vo}, and the ratio of the gas outlet and gas inlet CO_2 mole fractions, a_V:

$$\dot{n}_C = n_V Q_V Y_{Vo} \frac{(1 - a_V)}{(1 - Y_{Vo})}$$

So, eliminating the absorption rate between these two relations gives an equation for the maximum possible gas volume flow rate, Q_V^*, that can be handled by a given liquid flow rate and amine composition while reaching purification a_V.

$$Q_V^* = \frac{n_L Q_L}{n_V} \frac{(1 - Y_{Vo})}{(1 - a_V)} \left[\frac{a_A}{\alpha} + \frac{1}{f'} \right] \tag{3}$$

The parameter a_A is simply the non-dimensional amine mole fraction in the liquid: $a_A = Y_A / Y_{Vo}$. As mentioned, the equilibrium factor α varies with mole fraction of initial DEA and partial pressure of CO_2 in the gas (which varies along the contacting direction). Equilibrium can be approached at the inlet gas composition which corresponds to the liquid outlet for counter-current flow. Since high CO_2 partial pressure corresponds to low values of α, and hence more CO_2 absorbed per amine molecule, counter-current flow allows the liquid to hold more CO_2 at outlet than with a co-current arrangement. The function $\alpha(Y_A)$ used here for calculations with Eq. 3 is a power law function fit to the data of Lee et al. [16] interpolated to the spiral temperature and to the inlet value of CO_2 gas mole fraction ($\alpha = 2.54\, Y_A^{0.131}$). The constant f' is the slope of the equilibrium curve for dilute concentrations of CO_2 in the gas-water system, i.e. the ratio of gas and water mole fractions of CO_2. A value of $f' = 1270$ can be estimated from standard data at the conditions of the present experiments (1.8 bara and 312 K).

The upper limit of gas flow rate given by Eq. 3 will only be reached if there is sufficient time for diffusion to allow access to all parts of the liquid and for the reaction to progress so that further CO_2 can be absorbed. During passage of the liquid from inlet to outlet it flows in a layer of depth h_L that remains constant and can be estimated using the wide-channel model [2]. Given the liquid flow rate, the average velocity in the liquid layer, $u_L = Q_L / h_L w$, is determined for the known channel width, w, and hence the average time, $t = L/u_L$, taken for the liquid to flow along the contacting length, L, can be found. The characteristic diffusion layer depth in the liquid when it has reached the outlet can then be calculated from:

$$\delta = \sqrt{tD_L} \tag{4}$$

If the residence time of the liquid is too small, only a fraction of the liquid layer can be utilised for absorption and the treated gas flow rate in Eq. 3 is reduced by a factor depending on the ratio of the diffusion depth and the liquid layer thickness, δ/h_L. This takes no account of structural changes to the diffusion layer associated with reaction or when the diffusion depth becomes significant in comparison with the liquid layer thickness itself. Noting that the fraction of the liquid layer used must approach unity for diffusion depth larger than the liquid layer thickness itself, a suitable relation for the fraction of the layer accessed by diffusion, η, is given by

$$\frac{\eta}{1-\eta} = A\frac{\delta}{h_L} \tag{5}$$

The coefficient A adjusts the characteristic depth, δ, to an effective diffusion depth. The diffusion of DEA towards the reaction zone is closely similar to the case of diffusion without reaction in a liquid layer beginning with a uniform initial concentration and subject to zero concentration at the interface. Initially, the diffusion layer grows from the interface into an approximately infinite layer, for which the analytical solution [22] gives an effective layer thickness of $A\delta = 2\sqrt{tD_L/\pi}$ and thus, comparing with Eq. 4, $A = 2/\sqrt{\pi}$. This is approximate both since reaction is not directly accounted for and because it ignores the decreasing liquid velocity with depth. Also, as the diffusion layer growth fills the liquid layer the solution no longer applies; but in that limit the form introduced in Eq. 5 is arguably more important than the particular value used for A. Now the actual gas flow rate handled, Q_V, can be estimated by adjusting the maximum value, given by Eq. 3, by the available liquid fraction, η:

$$Q_V = \eta\, Q_V^* \tag{6}$$

Eq. 6 with Eq. 5 and the parameter values given will be used to aid interpretation of the experimental results.

2.2 Liquid layer scaling

The DEA-water mixtures become increasingly viscous as the DEA fraction increases, approaching around 900 times the viscosity of water for pure DEA at 20 °C (Arachchige et al. [23]). This increasing liquid viscosity with DEA concentration affects the mass transfer process since both the diffusion coefficient decreases and the liquid layer thickness increases. With the rotating spiral it is possible to operate with constant liquid layer thickness across the entire range of liquid viscosity and this constant liquid layer thickness also turns out to coincide with an approximately constant diffusion layer depth, hence a constant fraction of the liquid layer accessed by diffusion. This can be shown by considering the scaling of liquid layer thickness and average liquid velocity, as follows.

At the relatively low gas flow rates that will be required, the liquid layer is largely unaffected by the shear stress exerted by the gas at the phase interface [1]. Consequently, force on the liquid from the shear stress at the channel wall alone must balance the body force associated with centrifugal acceleration. Using this balance and the relation between average liquid velocity (u_L), layer thickness (h_L) and volume flow rate (Q_L), the following scaling relations at fixed rotation rate are found for u_L and h_L in terms of the liquid flow rate and liquid viscosity, μ_L.

$$u_L \propto \frac{Q_L^{2/3}}{\mu_L^{1/3}} \tag{7}$$

$$h_L \propto (\mu_L Q_L)^{1/3} \tag{8}$$

The relation for diffusion depth (Eq. 4) can now be expressed in terms of liquid flow rate and viscosity using Eq. 7 for u_L and the Stokes-Einstein dependence of diffusion coefficient on viscosity, $D_L \propto \mu_L^{-1}$.

$$\delta \propto (\mu_L Q_L)^{-1/3} \tag{9}$$

Thus, both h_L and δ depend on the product $\mu_L Q_L$ and so each remains constant if flow rate is varied inversely with viscosity, i.e. $Q_L \propto \mu_L^{-1}$. The constancy of h_L for fixed $\mu_L Q_L$ has been demonstrated experimentally by MacInnes and Zambri [1]. The measured layer thickness over a range of liquid flow rate and for liquids with viscosities ranging from 0.0006 to 0.06 Pa s collapsed when plotted against $\mu_L Q_L$. The initial experiments here are conducted such that the liquid layer thickness remains approximately 86 μm by varying the liquid flow rate inversely with viscosity, as the DEA mole fraction is changed. Since this results in both constant liquid layer thickness and constant diffusion layer depth, according to Eq. 9, the fraction of the liquid layer accessed by diffusion, δ/h_L, also remains constant as mixture composition is varied.

3. Experiment

The apparatus used in this work was first reported in MacInnes and Zambri [1]. Briefly, two fluid phases are transferred continuously to and from the rotating spiral channel through pairs of lip seals to make flow connections with the rotating unit. Fig. 1 shows a schematic diagram of the flow system. Rotation rate is adjustable along with the flow rates of the fluid phases, which are changed by adjusting the driving pressures (regulator REG 1 for gas phase and REG 2 to drive liquid phase from a bottle in the pressure pot) and the needle valve setting at the gas phase outlet. Temperature in the spiral is determined by the balance between heat

generated by the shaft bearings and the seals and the heat lost to the ambient (including to cooling water flowing through longitudinal passages in the shaft). MacInnes and Zambri established a correlation between rotation rate and the temperature in the spiral channels and this relation is used here to estimate spiral temperature. The spiral element is the same one used in the previous work, having a rectangular flow section 1.5 mm by 4.0 mm and 900 mm in length. The liquid outlet path serves as a manometer to determine the spiral pressure. All experiments reported here use a rotation rate of 3200 rpm with the liquid outlet to atmospheric pressure for which conditions the estimated temperature and pressure in the spiral are 312 K and 1.8 bara absolute. This rotation rate is sufficiently high for the end menisci to have negligible influence on liquid layer thickness so the wide channel model [2] gives a reliable representation [1].

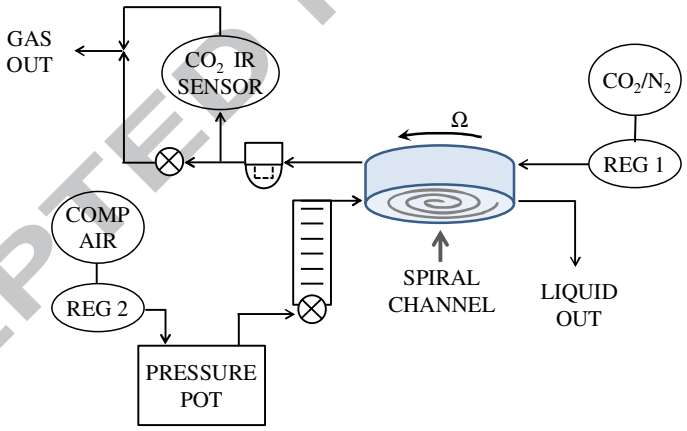

Figure 1. Flow and sensing arrangement.

Flow rates in the experiments ranged over about three orders of magnitude for the gas and two orders of magnitude for the liquid. Two separate outlet paths passing through two

separate needle valves were used to span the gas flow range. The low gas flow rate path was used for flow rates from 1 NmL/min up to 70 NmL/min. The second path was used for flow rates from 70 NmL/min up to 3 NL/min. The flow system for the high flow rate path is depicted in Fig. 1. In that case, the outlet gas is split with only part of the flow passing through the sensor, the rate governed by a capillary channel to avoid high pressure in the sensor. The low flow arrangement differed in that the entire outlet gas flow passed through the sensor. Gas was supplied from a regulated gas bottle delivering an approximately 10% CO_2 mixture with N_2. Gas flow rates were determined by timed collection of gas volume at the outlet in an upturned graduated cylinder immersed in a sink filled with water. The water and ambient air were within a few degrees of 20 °C and the cylinder gas volume was read with the liquid level within a few centimetres of the sink level; thus the flow rate recorded was volume of gas at 20 °C and atmospheric pressure, hence normal flow rate.

In the case of the liquid, a syringe pump was used at flow rates below 1 mL/min where the flow rate was determined from pump speed and syringe size. At higher flow rates, the liquid was supplied from a bottle in an air-pressurised 'pot' (Fig. 1) and flowed through a needle valve and rotameter. The needle valve was left fully open and flow rate was adjusted using the pot pressure. Syringe flow rates and rotameter flow rates were checked directly by collecting liquid at the outlet in a vile for a measured time. This liquid was weighed and the mass converted to volume using data for density of DEA-water mixtures (Rinker et al. [24]).

The principal difference from the apparatus described in MacInnes and Zambri [1] is the insertion of the sensor to measure CO_2 composition. Depending on the configuration, all or part of the outlet gas flow is passed through an infra-red sensor (CO2S-FR-X, SST Sensing Ltd.) to record CO_2 mole fraction. The standard software supplied with the sensor was used both to indicate the reading and to zero the sensor in the presence of N_2. Zeroing was performed when the reading for the air, used to dry the apparatus when not in use, drifted by

more than about 0.2% of the maximum CO_2 mole fraction. The supply gas composition used throughout the tests was that produced directly from the nominally 0.1 mole fraction CO_2 bottle. In practice the CO_2 mole fraction delivered by the bottle at the beginning of an experimental session agreed to within 2% of the value measured several hours later, at the end of the session; over the course of the experiments the delivered composition rose somewhat as the bottle gradually emptied.

The gas exiting the spiral can be assumed to be saturated with water at the spiral temperature, which corresponds to a water mole fraction of 0.039 in the outlet gas. To prevent condensation in the sensor, the sensor and tubing just upstream were heated such that the sensor outlet reached 30 °C. While this is below the dew point at the spiral pressure, at the lower pressure within the sensor (atmospheric) this temperature is above the dew point and condensation is prevented.

The downstream sensor was used to measure both upstream and downstream CO_2 mass fractions. During the initial warmup period following the start of rotation, no liquid is allowed to flow in the spiral while the bottle gas supply is flowing through the spiral to the downstream sensor. Since no take-up of CO_2 occurs once any of the fixed material along the path equilibrates with the supply composition, the gas outlet composition at the sensor will be the same as that at the inlet. When the liquid flow is started the sensor then records the reduced CO_2 composition from absorption of the outlet gas.

In all cases, the gas composition measurement was made only after steady conditions of the flow and composition fields in the spiral and throughout the downstream passage leading to the sensor were reached, so the CO_2 composition of the gas in the sensor could be taken as identical to that in the gas exiting from the spiral. It was found that approximately 20 downstream passage volumes of gas flow were required to establish the correct composition

from the spiral gas outlet through to the sensor. Thus, high gas flow rate required shorter time to establish correct composition and low gas flow rate longer. In the case of the low flow range it was essential to reduce downstream passage volume to a minimum to avoid excessive waiting time. For this purpose, the entire outlet gas flow was directed through the sensor and all unnecessary downstream fittings and volumes were eliminated. A downstream passage volume of about 3 mL was reached requiring one hour for a valid sensor reading in the case of the lowest gas flow rate of 1 NmL/min. For the higher flow rate range, the downstream volume was around 30 mL as a result of the filter placed upstream of the sensor and needle valve (Fig. 1). This filter is essential to handle the greater volume of condensing water at the high gas flow rates and to prevent this liquid from entering either the needle valve or the sensor.

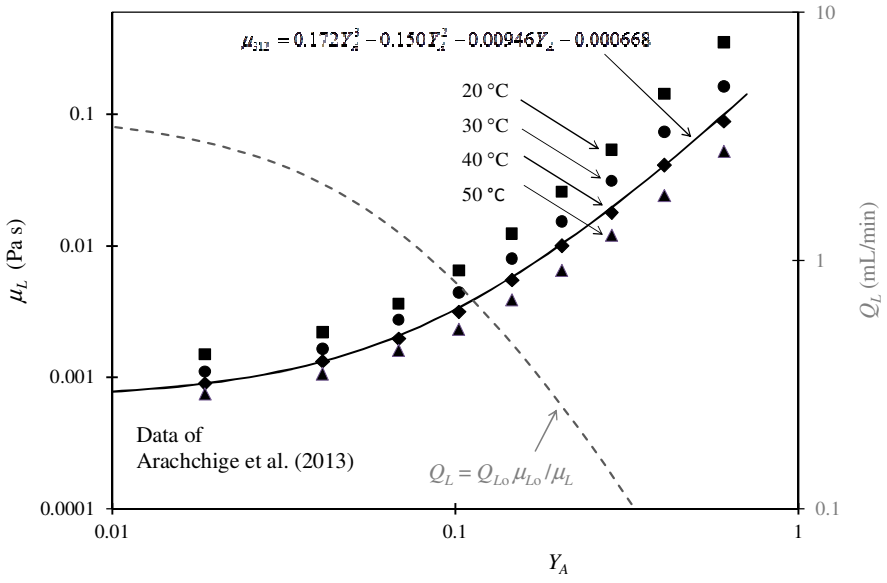

Figure 2. Viscosity data from Arachchige et al. [23] for DEA-water mixtures at four temperatures. The solid curve is a fit to the data interpolated to the spiral temperature (312 K) for the experimental rotation rate (3200 rpm). The dashed curve shows the required

variation of liquid flow rate to maintain a constant liquid layer thickness (86 μm) and diffusion depth.

In order to maintain a constant fraction of liquid layer access as the DEA composition is varied in the experiments, the flow rate of liquid must be changed in relation to the liquid viscosity as indicated in Section 2.2. Thus, liquid viscosity at the spiral temperature must be known as a function of DEA mole fraction in the liquid. Fig. 2 shows viscosity data from Arachchige et al. [23] at four temperatures over the range of DEA mole fraction. The solid line is a cubic polynomial fit to the data interpolated to the spiral temperature (312 K). Over the range of the experimental compositions (0 to 0.25 mole fraction DEA) the viscosity increases by a factor of 24 according to the data. In order to maintain constant liquid layer thickness and diffusion depth, the liquid flow rate is varied inversely with viscosity and the corresponding function of DEA mole fraction is shown on the plot as a dashed line. In the experiments, the liquid layer thickness of about 86 μm is established using reference values μ_{Lo} = 1.01×10^{-3} Pa s and Q_{Lo} = 2.65 mL/min (pure water at 20 °C). These values derive from the liquid layer thickness measurements of MacInnes and Zambri [1].

4. Results

Figs. 3 and 4 present purification results (a_V) as a function of gas flow rate for a series of different DEA mixtures. The liquid flow rate for each mixture was selected to maintain uniform liquid layer thickness and diffusion depth, as discussed in Section 2, but using a rough approximation for viscosity of the liquid mixtures (not that in Fig. 2). The different mixture compositions are divided into two plots with Fig. 3 including the relatively low DEA

concentrations and Fig. 4 the higher concentrations. For each composition, a_V evidently decreases and approaches zero as the gas flow rate decreases, so that any given degree of purification can be reached by sufficient reduction in gas flow.

For DEA mole fractions up to 0.064 (28% by mass), shown in Fig. 3, the gas flow rate that can be handled while maintaining a given purification increases with the mole fraction of DEA as there is increasing flow rate of DEA. Fig. 4 shows that beyond a mole fraction of 0.064 the amount of gas that can be handled ceases to increase and in fact begins to decrease with further increase in DEA concentration. While the amount of DEA in the liquid layer continues to increase with concentration, the viscosity of the liquid increases more rapidly than before and the required reduction in liquid flow rate leads to a decrease in DEA flow rate and, hence, in the capacity to absorb CO_2.

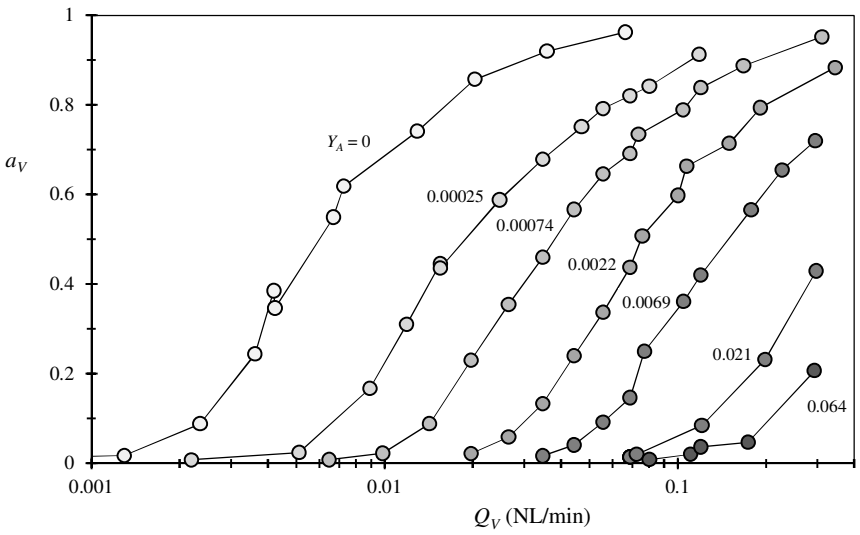

Figure 3. Measured purification as a function of gas flow rate for DEA mixtures in the range 0 to 0.064 mole fraction (0 to 0.28 mass fraction). Liquid flow rate is adjusted to maintain constant liquid layer thickness of 86 µm.

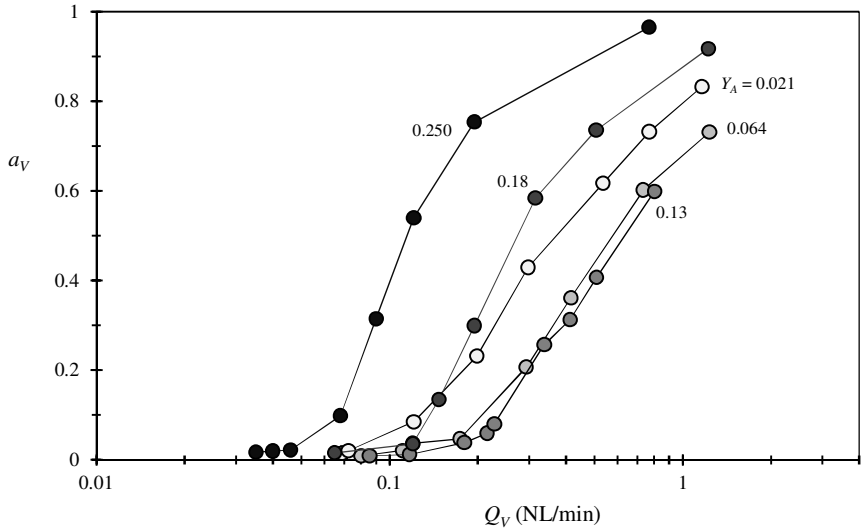

Figure 4. As Fig. 3 but for DEA mole fraction range 0.021 to 0.25 mole fraction (0.11 to 0.66 mass fraction).

This behaviour can be captured more clearly in a plot of gas flow rate for constant purification, where comparison with the estimate of maximum gas flow rate can also be made. At this stage, it was found that the rough approximation for the liquid viscosity led to a significant underestimate of liquid flow rate at high concentrations of DEA. Tests over the affected mole fraction range ($Y_A \geq 0.05$) were thus repeated using the liquid flow rates according to the correct viscosity (Fig. 2). Fig. 5 shows the result for the case of 90% removal of the CO_2 ($a_V = 0.1$). (The experimental values of Q_V are determined by fitting a quadratic polynomial to several data at different Q_V in the vicinity of the target purification and interpolating.) The peak in the measured gas flow rates (symbols) is quite broad, remaining within 10% of the maximum value (221 NmL/min) for DEA mole fraction in the range 0.04 to 0.1 (20 to 40% by mass). It can be noted that the peak gas flow rate is about two orders of magnitude greater than the flow that can be treated to the same purity using

water alone (the horizontal short dashed line near the bottom of the figure). The maximum possible gas flow rate (Q_V^*, Eq. 3) is plotted as a solid curve and shows that the DEA has not been fully utilised: the measured gas flows are about 30% of those possible, although this increases to around 70% at the higher DEA concentrations. The shape of the curve and the reduced utilisation is partially captured by including the estimate taking account of diffusion layer depth (Eq. 6 with Eq. 5). The dark dashed curve shows this adjustment to allowed gas flow rate and at the higher DEA concentrations this makes up for the difference. At low concentrations, the residence time of the liquid is shorter since liquid flow rates are higher with these lower viscosity solutions. It is found that multiplication by an exponential function of residence time that attenuates the absorption for short times can account for the measurements:

$$Q_V = \eta\, Q_V^* \left[1 - \exp(-t/\tau)\right] \qquad (10)$$

Eq. 10 produces the grey dashed curve in Fig. 5 when τ is adjusted to give least-squared error with the data (τ = 10.2 s). The skewing of the peak in the measured values to larger concentration compared with the maximum flow estimate is the consequence of whatever effects this exponential correction represents.

It can be noted that the result at the lowest DEA concentration shown is nearer to the estimate without the exponential factor (dark dashed curve). Results at still lower DEA concentration (not shown on the plot) are similarly nearer. It is not known why this is found, although it can be noted that the liquid Reynolds number rises here to a level (>20) where convective effects may have an influence.

Finally, at the two highest concentrations measured, the data suggest a greater utilisation than for the estimated diffusion depth. The implied under-estimation of diffusion depth may be due in part to the use of the Stokes-Einstein relation to represent the decrease in diffusion

coefficient with viscosity. Measured values of DEA diffusion coefficient [25] show a less rapid decrease with increasing viscosity than given by the Stokes-Einstein relation and this could explain the too low levels of Q_V estimated at the two highest values of Y_A in Fig. 5.

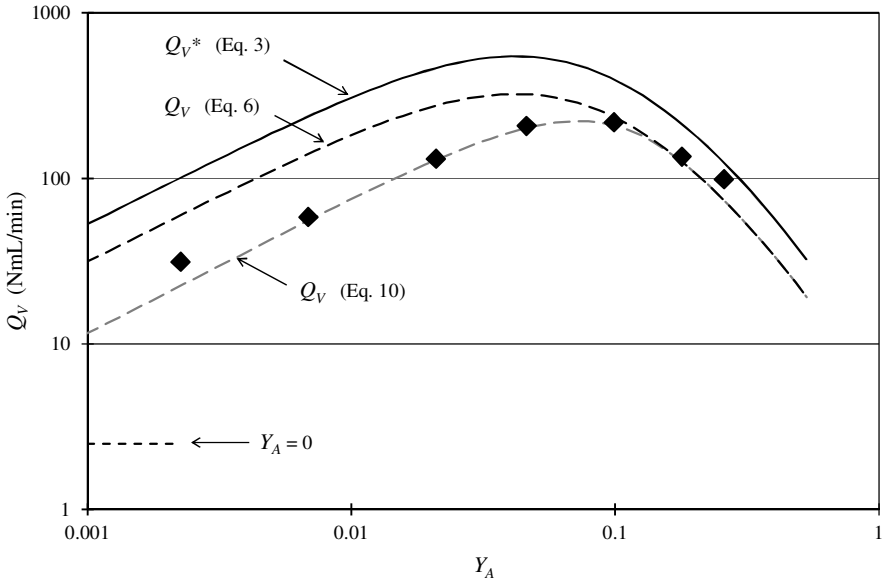

Figure 5. Measured gas flow rate (for $a_V = 0.1$) as a function of DEA mole fraction in the liquid. The solid curve is the theoretical limit of CO_2 absorption (Eq.3); the dark dashed curve is Eq. 6 using Eq. 5 and the light dashed curve includes the exponential function of residence time.

4.1 Optimum composition

An important practical issue is identifying the optimum DEA composition. Two possible objectives may usefully be considered: maximising the gas flow rate per device size and maximising the gas flow rate per DEA consumed. The first minimises device size and the second minimises DEA flow rate for a given throughput (flow rate) of treated gas. In simple

terms, the device size may be taken as proportional to liquid volume within the contactor, so minimum device size corresponds to maximum gas flow rate per liquid volume in the contactor. Minimum DEA use, on the other hand, corresponds to maximum gas flow rate per DEA flow rate.

Since, for the results in Fig. 5, the volume of liquid is fixed (h_L is constant and the spiral channel length and width are not changing) the minimum device size corresponds to the maximum treated gas flow rate, which is at a DEA mole fraction of 0.072 (31% by mass) using the maximum of the fitted function (grey dashed curve in Fig. 5). But, as has been mentioned, the peak is quite flat so a DEA composition within a broad range may be acceptable in practice. On the other hand, if minimising the use of DEA is the objective, the maximum treated gas flow rate per DEA flow rate is required and this occurs when the layer is fully utilised. Since the fraction utilised increases with DEA concentration (Fig. 5) the best concentration of DEA to use in that case would appear to be the largest, in the range covered by the data. However, the increase with DEA mole fraction becomes marginal beyond about $Y_A = 0.17$ (according to the fitted function) and clearly also there is a balance between DEA use and device size. Further, it may be possible to increase the layer use in the vicinity of the gas flow rate peak by reducing liquid layer thickness and this is considered next.

For any DEA composition, the fraction of the liquid accessed by diffusion can be increased by reducing the liquid flow rate. The diffusion depth increases since the average velocity is decreased (Eq. 7), allowing more time for diffusion to occur, and this increased depth is a greater fraction of the decreased liquid layer thickness (Eq. 8). Fig. 6 shows the result of varying the liquid flow rate for a fixed DEA mole fraction of 0.021. Again Q_V^* is plotted along with the estimates for Q_V (both with and without the exponential factor, again the grey and dark dashed curves, respectively). As before, the data are captured well when the

exponential factor of residence time is included (value of τ as before). The estimate successfully reproduces the order of magnitude lower gas flow rate relative to Q_V^* found in the data at large liquid flow rate, i.e. small residence time. This reduction is clearly the result of the exponential factor of residence time (grey dashed curve), since the finite depth of the diffusion layer accounts for only a 40% reduction from maximum utilisation (dark dashed curve). On the other hand, decreasing the liquid flow rate leads as expected to increasingly full use of the DEA, and the data approach the Q_V^* line as Q_L is decreased. The approach to equilibrium appears quite slow, however, and this may be partly due to the fact that at the early stages of contacting the liquid is exposed to gas with much lower gas CO_2 partial pressure, for which the equilibrium value of α is about 50% higher than that at the inlet gas composition. It is also possible that the actual spiral temperature is somewhat higher than estimated. The resulting increase in α would drop the Q_V^* estimate in the direction of the data.

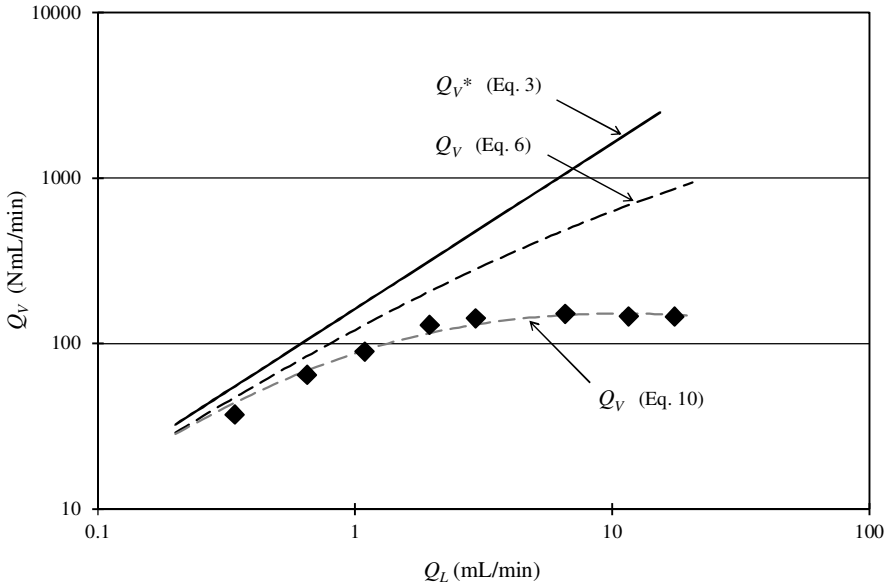

Figure 6. Variation of measured gas flow rate (for $a_V = 0.1$) with liquid flow rate using a 0.021 mole fraction DEA liquid mixture. Curves as defined for Fig. 5.

The data in Fig. 6 show that the maximum flow rate of treated gas occurs at somewhat higher liquid flow rate than was used in Fig. 5 at this DEA mole fraction (2.93 mL/min), although the improvement is marginal. Thus, the maximum treated gas flow rate per liquid volume identified from the results in Fig. 5 looks unlikely to change with further exploration.

In the case of minimising the DEA consumed, the gas flow rate per DEA flow rate continues to increase as Q_L is reduced, as complete utilisation of the DEA in the liquid is approached. Although, again, full utilisation comes at the expense of decreasing gas throughput per liquid volume and hence increasing device size. This is because the gas flow rate decreases in proportion to Q_L (assuming full utilisation) and the liquid volume decreases in proportion to $h_L \propto Q_L^{1/3}$, so gas flow rate decreases more rapidly than liquid volume as the liquid flow rate is decreased.

5. Discussion and conclusions

A rotating spiral channel has been used here both to produce effective mass transfer and to explore optimum contacting conditions for the removal of CO_2 from a nitrogen gas stream using aqueous mixtures of diethanolamine (DEA). Results are obtained over the range of composition up to 67% (mass) DEA. When the liquid flow rate is adjusted for viscosity to maintain constant liquid layer thickness, it is shown theoretically that also the characteristic layer depth that can be reached by diffusion during contacting of the liquid is also constant. It is argued that conducting experiments with constant layer thickness and diffusion depth allows identification of the optimum DEA composition, since the fraction of the DEA that is accessible is the same regardless of composition.

The measured gas flow rate for 90% removal of the CO_2 is found to have a maximum at 31% DEA by mass, although the peak is quite broad and compositions in the range 20 to 40% allow the same purification with at most 10% reduction in the gas flow rate. Since the liquid layer thickness remains constant in these tests, the flow rate per volume of liquid is also maximum where the gas flow rate peaks and is 12 Nm^3/s per cubic metre of liquid (from Fig. 5 and for the liquid layer thickness and channel width used). The size of the contacting equipment, when well designed, is proportional to the liquid volume within and thus this maximum represents the condition of minimum device size. Thus, the determination of optimum treated gas flow rate per liquid volume for different absorbent blends using a rotating spiral channel allows quantification of the relative device size required for a given blend. This information can be combined with details concerning regeneration costs and other considerations to identify absorbent liquid formulations giving optimum performance overall. A second processing objective may be to use the minimum amount of DEA to treat a

given volume of gas. This condition requires full utilisation of the DEA. It is shown by varying the liquid flow rate, and hence liquid layer thickness and average liquid velocity, that full use of the DEA is approached. However, the device size is increased significantly relative to the minimum achievable.

A simple approximation for the treated gas flow rate is constructed using an estimate of the fraction of the layer accessible by diffusion. It is found that an exponential function of liquid residence time is needed to match the data. The physical mechanism represented by this function of residence time is not yet clear and its use can only be justified at present by the close fit to the data it produces and the apparent implication which follows: that diffusion scaling alone does not account for the observed behaviour. A number of factors can be identified which may explain this observed time-dependent behaviour. However, by exclusion it seems most likely that this observed effect stems from the array of competing reaction equilibria that exist between the DEA, water, CO_2 and their resultant products over the timescales and conditions experienced on the spiral contactor.

It is clear that the rotating spiral apparatus has allowed effective identification of optimum absorption characteristics using aqueous DEA as the absorbent. The essential results presented required about five hours of experimental time to collect. It is clear that the same device could be used to explore wide ranges of amine types and blends of these and other components in the same way as was done here. It is noted also that the present device has been designed for general purpose use and it would be possible now to specialise the design to achieve reduced sample times and to allow testing over a range of temperature and pressure conditions.

Acknowledgements

We thank the Iraqi Government for an HCED Scholarship (D 11-3508) supporting AAA and the EPSRC for 4CU Programme Grant funding (EP/K001329/1) at The University of Sheffield supporting GRMD. Some of the data were collected with the help of Vito Carella, Wenhan Dai and Ji Lyu during their MSc research project work at The University of Sheffield.

References

[1] J.M. MacInnes, M.K.S. Zambri, 2015, Hydrodynamic Characteristics of a Rotating Spiral Fluid-phase Contactor, Chem. Eng. Sci., 126, 427-439.

[2] J.M. MacInnes, M.J. Pitt, G.H. Priestman, R.W.K. Allen, 2012, Analysis of Two-phase Contacting in a Rotating Spiral Channel, Chem. Eng. Sci., 69, 304-315.

[3] G. Rochelle, E. Chen, S. Freeman, D. van Wagener, Q. Xu, A. Voice, 2011, Aqueous Piperazine as the New Standard for CO_2 Capture Technology, Chem. Eng. J., 171, 725-733.

[4] L. Raynal, P.-A. Bouillon, A. Gomez, P. Broutin, 2011, From MEA to Demixing Solvents and Future Steps, a Roadmap for Lowering the Cost of Post-Combustion Carbon Capture, Chem. Eng. J., 171, 742-752.

[5] G. Puxty, R. Rowland, A. Allport, Q. Yang, M. Bown, R. Burns, M. Maeder, M. Attalla, 2009, Carbon Dioxide Postcombustion Capture: A Novel Screening Study of the Carbon Dioxide Absorption Performance of 76 Amines, Environ. Sci. Technol., 43, 6427-6433.

[6] S. Ma'mum, H.F. Svendsen, K.A. Hoff, O. Juliussen, 2007, Selection of New Absorbents for Carbon Dioxide Capture, Energy Conversion and Management, 48, 251-258.

[7] T. Sema, A. Naami, K. Fu, M. Edali, H. Liu, H. Shi, Z. Liang, R. Idem, P. Tontiwachwuthikul, 2012, Comprehensive Mass Transfer and Reaction Kinetics Studies of

CO_2 Absorption into Aqueous Solutions of Blended MDEA-MEA, Chem. Eng. J., 209, 501-512.

[8] G. Richner, G. Puxty, A. Carnal, W. Conway, M. Maeder, P. Pearson, 2015, Thermokinetic Properties and Performance Evaluation of Benzylamine-Based Solvents for CO_2 Capture, Chem. Eng. J., 264, 230-240.

[9] W. Conway, Y. Beyad, G. Richner, G. Puxty, P. Feron, 2015, Rapid CO_2 Absorption into Aqueous Benzylamine (BZA) Solutions and its Formulations with Monoethanolamine (MEA), and 2-amino-2-methyl-1-propanol (AMP) as Components for Post Combustion Capture Processes, Chem. Eng. J., 264, 954-961.

[10] B. Lv, Y. Shi, C. Sun, N. Liu, W. Li, S. Li, 2015, CO_2 Capture by a Highly-Efficient Aqueous Blend of Monoethanolamine and a Hydrophilic Amino Acid Ionic Liquid [C_2OHmim][Gly], Chem. Eng. J., 270, 372-377.

[11] A. Aroonwilas, A. Veawab, 2004, Characterisation and Comparison of the CO_2 Absorption Performance into Single and Blended Alkanolamines in a Packed Column, Ind. Eng. Chem. Res., 43, 2228-2237.

[12] A. Chakma, E. Chornet, R.P. Overend, W.H. Dawson, 1990, Absorption of CO_2 by Aqueous Diethanolamine (DEA) Solutions in a High Shear Jet Absorber, Can. J. Chem. Eng., 68, 592-598.

[13] J. Hu, J. Liu, J. Yu, G. Dai, 2013, CO_2 Absorption into Highly Concentrated DEA Solution Flowing over a Vertical Plate with Rectangular Windows, Int. J. Greenh. Gas Control, 19, 13-18.

[14] E.B. Rinker, S.S. Ashour, O.C. Sandall, 1996, Kinetics and Modeling of Carbon Dioxide Absorption into Aqueous Solutions of Diethanolamine, Ind. Eng. Chem. Res., 35, 1107-1114.

[15] J.W. Mason, B.F. Dodge, 1936, Equilibrium Absorption of Carbon Dioxide by Solutions of the Ethanolamines, Trans. AIChE, 32, 27-48.

[16] J.I. Lee, F.D. Otto, A.E. Mather, 1972, Solubility of Carbon Dioxide in Aqueous Diethanolamine Solutions at High Pressures, J. Chem. Eng. Data, 17 (4), 465-468.

[17] M.Z. Haji-Sulaiman, M.K. Aroua, A. Benamor, 1998, Analysis of Equilibrium Data of CO_2 in Aqueous Solutions of Diethanolamine (DEA), Methyldiethanolamine (MDEA) and Their Mixtures Using the Modified Kent Eisenberg Model, Trans. IChemE, 76, Part A, 961-968.

[18] D.W. van Krevelen, P.J. Howtijzer, 1948, Kinetics of Gas-Liquid Reactions, Part I. General Theory, Recueil des Travaux Chimiques des Pays-Bas, Tome 67, Neth. Chem. Soc., 563-586.

[19] P.V. Danckwerts, 1950, Unsteady-state Diffusion or Heat-Conduction with Moving Boundary, Trans. Faraday Soc., 46, 701-712.

[20] E.R. Gilliland, R.F. Baddour, P.L.T. Brian, 1958, Gas Absorption Accompanied by a Liquid-phase Chemical Reaction, AIChE J., 4 (2), 223-230.

[21] P.L.T. Brian, J.F. Hurley, E.H. Hasseltine, 1961, Penetration Theory for Gas Absorption Accompanied by a Second Order Chemical Reaction, AIChE J., 7 (2), 226-231.

[22] P.V. Danckwerts, 1970, Gas-Liquid Reactions, McGraw-Hill.

[23] U.S.P.R. Arachchige, A. Neelakantha, D.A. Eimer, M.C. Melaaen, 2013, Viscosities of Pure and Aqueous Solutions of Monoethanolamine (MEA), Diethanolamine (DEA) and N-Methyldiethanolamine (MDEA), Annu. Trans. Nordic Rheol. Soc., 21, 299-306.

[24] E.B. Rinker, D.W. Oelschlager, A.T. Colussi, K.R. Henry, O.C. Sandall, 1994, Viscosity, Density, and Surface Tension of Binary Mixtures of Water and N-

Methyldiethanolamine and Water and Diethanolamine and Tertiary Mixtures of these Amines with Water over the Temperature Range 20-100 °C, J. Chem. Eng. Data, 39, 392-395.

[25] H. Hikita, H. Ishikawa, K. Uku, T. Murakami, 1980, Diffusivities of Mono-, Di-, and Triethanolamines in Aqueous Solutions, J. Chem. Eng. Data, 25, 324-325.

CO_2 Absorption Using Diethanolamine-Water Solutions in a Rotating Spiral Contactor

Jordan M. MacInnes, Ahmed A. Ayash and George R. M. Dowson

Highlights

- CO_2 absorption in a rotating spiral channel
- Rapid and facile determination of optimum absorbent composition
- Precise control of contacting over a wide range of absorbent blends
- Elementary theoretical framework used to describe contacting parameters
- Demonstration using aqueous diethanolamine solutions